Simulation of below-gap photoresponse of thin-film superconductors by Josephson-junction arrays

Y. Cai and P. L. Leath
Department of Physics and Astronomy, Rutgers, The State University, Piscataway, New Jersey 08855-0849

Z. Yu
Center for Computer Aids to Industrial Productivity, Rutgers University, Piscataway, New Jersey 08855-1390
(Received 10 June 1993)

The below-gap, nonbolometric photoresponse of granular, thin-film superconductors seen recently by Strom *et al.* and by other experimental groups is simulated by a numerical study of the dc voltage response to an applied ac current at finite temperature, by ordered and disordered two-dimensional arrays of resistively shunted Josephson junctions. The current-assisted random generation of vortex-antivortex pairs by the temperature fluctuations and the ac current is observed. The photoresponse for perfect arrays shows a large peak at the Kosterlitz-Thouless transition T_{KT} which moves to lower temperature with increasing I_{dc} or I_{ac}. For randomly diluted, disordered arrays at $p=0.9$ (10% of the junctions removed) the peak in the photoresponse is greatly enhanced and moved to lower temperatures. The behavior of the photoresponse versus bias current, ac power, and frequency is reported. A simple model of random localized heating is tried as a numerical approach to explain some features of the above-gap photoresponse.

I. INTRODUCTION

Recent experiments have demonstrated the large, nonbolometric photoresponse of superconducting thin films. These experiments have been motivated by possible applications to high-speed radiant energy detection in the far infrared. This large nonbolometric photoresponse was reported for thin, high-resist superconducting thin films by Bertin and Rose over twenty years ago.[1] More recently the phenomenon has been studied in two-dimensional (2D) granular films of Sn,[2] NbN,[3,4] NbN/BN,[5] $BaPb_{0.7}Bi_{0.3}O$,[6] $Bi_2Sr_2CaCuO_8$,[7] and $YBa_{2.1}Cu_{3.4}O_{7-x}$.[8-10] The general features of the nonbolometric photoresponse in all of these granular materials are the same. The purpose of the numerical simulations reported here is to elucidate the general nature of this photoresponse and its relation to vortex depinning and depairing.

Granular superconductors consist of superconducting grains connected by intergrain tunneling through weak links.[11] These weak links can be modeled by arrays of tunnel junctions.[4] For overdamped systems, such as thin, superconducting films, these links can be modeled by resistively shunted Josephson-(RSJ-) junction arrays.[12] Furthermore, the new high-T_c ceramic superconductors, especially in their polycrystalline form, behave in many ways like random arrays of weak links.[13]

In this paper we extend the studies reported earlier[14,15] to finite temperatures and to the presence of high-frequency ac currents in order to simulate the below-gap photoresponse. We consider two-dimensional arrays of superconducting grains which are located on the sites (nodes) of a square lattice. Each node is connected to its nearest neighbors by bonds occupied by RSJ junctions. The RSJ junctions (bonds) are identical and disorder is introduced by randomly removing junctions (bonds). The numerical techniques used here are described in Ref. 15 (except for the finite-temperature extension) and are similar to those used by several previous authors.[16-18] Since it has become relatively routine to study the properties of Josephson-junction arrays experimentally,[19] photoresponse measurements on such arrays should be possible so that the phenomena described here could also be seen in those systems.

In Sec. II we introduce the model by describing the case of a single RSJ junction, which has been solved analytically at finite temperature.[20] The numerical method is described and the numerical results are presented and compared with the exact analytic results, in the case of no applied ac current, as a check of the numerical simulation. In Sec. III, we describe our results for the photoresponse of a perfect array which displays the depairing of vortex-antivortex pairs by the temperature and by the applied ac current. Following that we study the response of samples with defects and discuss the enhancement effect caused by the vortex depinning process at the defects. Also, we briefly attempt a simulation to approximate the above-gap response signals.

II. THE MODEL

We assume that superconducting grains are occupying the sites of a square lattice. The state on each grain (site) is described by a complex superconducting order parameter $\Delta=\Delta_0 e^{i\phi}$ where Δ_0 is constant for all grains and the phase ϕ varies from grain to grain. Each grain is connected to each of its nearest neighbors by a resistively shunted Josephson (RSJ) junction (bond). At finite temperature, the shunt resistances will exhibit a fluctuating noise current I_{ij} which is approximated by the white-

noise form of Ambegaokar and Halperin[20] with the following statistical characteristics:

$$\langle \tilde{I}_{ij}(t) \rangle = 0 \tag{1}$$

and

$$\langle \tilde{I}_{ij}(t+\tau)\tilde{I}_{kl}(t) \rangle = \frac{2k_B T}{R_{ij}} \delta(\tau)\delta_{ij,kl} \ , \tag{2}$$

where $\langle\ \rangle$ denotes an ensemble average. With these assumptions, the noise currents in different shunt resistances are uncorrelated and the noise current in a single bond has zero correlation time corresponding to white noise (Josephson noise). Thus, the Josephson equations of motion for a single junction become

$$\frac{d}{dt}(\phi_i - \phi_j) = \frac{2e}{\hbar} V_{ij} \ , \tag{3}$$

and

$$I_{ij} = J \sin(\phi_i - \phi_j) + \frac{V_{ij}}{R} + \tilde{I}_{ij}(t) \ , \tag{4}$$

where the first term in Eq. (4) is the supercurrent due to the phase difference across the junction, and the second term is the normal current. The normal resistance is R and J is the critical supercurrent of the junction. The capacitive terms in the current have been neglected which is reasonable for proximity-effect junctions. We shall write all equations in reduced units, where the unit for time t is $\hbar/(2eRJ)$, the unit for current is J, and the unit for frequency f is $\hbar/eJR$. Equation (4) thus becomes

$$i_{ij} = \sin(\phi_i - \phi_j) + \frac{d}{dt}(\phi_i - \phi_j) + \tilde{i}(t) \ . \tag{5}$$

This single junction equation can be solved analytically,[21,22] at zero temperature to obtain, for $i > 1$,

$$V_{ij}(t) = \frac{(i^2-1)}{i + \sin[t(i^2-1)^{1/2}]} \ . \tag{6}$$

This result gives the form of the Josephson oscillations that appear for $i > 1$ with period $T_i = 2\pi/(i^2-1)^{1/2}$, and the average voltage as a function of i becomes

$$\langle V(i) \rangle = (i^2-1)^{1/2} \ . \tag{7}$$

When an external ac current is applied as well so that the total external current across the junction is

$$i^{\rm ext}(t) = i_{\rm dc} + i_{\rm ac} \cos(2\pi f t) \ , \tag{8}$$

there is an extra dc voltage $\langle \Delta V_R \rangle$ which appears across the sample; this voltage increment is called the photoresponse. This extra response to the ac current is discussed in detail by Kanter and Vernon[23] who derive the formula for the photoresponse at high frequency, which is

$$\langle \Delta V_R \rangle = C i_{\rm ac}^2 (i^2-1)^{-3/2}/(f^2-1) \ , \tag{9}$$

where $C = (1/16\pi^2)$. This high-frequency behavior is typical of systems being driven well beyond their natural resonant frequencies. When the temperature is not zero, Eq. (5) is solved for the average voltage by Ambegaokar and Halperin[20] by the introduction of a Fokker-Planck equation for the probability distribution for the phase $\phi_i(t)$ across the junction,

$$\langle V(i) \rangle = T A^{-1}(T)(1 - e^{-i\pi/T}) \ , \tag{10}$$

where

$$A(T) = \int_0^{2\pi} d\chi e^{-i\chi/(2T)} I_0(T^{-1} \sin\chi/2) \ .$$

It can be checked that Eq. (10) reduces to Eq. (7) in the limit $T \to 0$.

We next consider a perfect $N \times N$ array of junctions as illustrated in Fig. 1. The external current is applied to the array by injecting it at a single superconducting grain at the top of the sample and removing it from a similar grain at the bottom (Fig. 1). These two single grains serve as bus bars which distribute the current appropriately across the top and bottom of the $N \times N$ array. At each node (grain) of the array the z junctions come together and Eqs. (5) for each single junction are added to conserve current at the node. The resulting set of coupled equations at node k are

$$\sum_l \frac{d}{dt}(\phi_k - \phi_l) = i_k^{\rm ext} - \sum_l [\sin(\phi_k - \phi_l) + \tilde{i}_{kl}(t)] \ , \tag{11}$$

where $\tilde{i}_{kl}(t)$ is the white-noise current applied randomly to each junction in each time step, and where $i_k^{\rm ext}$ is generally zero everywhere except at the top and bottom bus bar sites. At the top and bottom bus bar sites the external current will generally include both a dc bias current and an ac current as given by Eq. (8). These equations of motion (11) can be collectively written in a generalized matrix form

$$M \frac{d\phi}{dt} = C(\phi) \ , \tag{12}$$

where $C(\phi)$ is the nonlinear term which includes the $\sin(\phi_k - \phi_l)$ terms of Eq. (11). In the next section we shall solve these equations numerically by inverting M to the right-hand side of Eq. (12) and integrating numerically.

The analytic solution of Eq. (12) is sufficiently difficult that it cannot be done exactly except in certain limiting

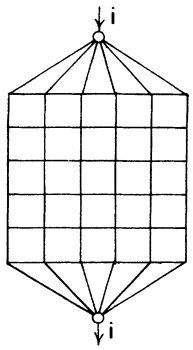

FIG. 1. A perfect $N \times N$ array of resistively shunted Josephson junctions connected to single superconducting grains at the top and bottom of the array, which act as bus bars.

situations. In particular, the behavior near the Kosterlitz-Thouless (KT) phase transition to the normal state has been studied in great detail.[24–26] The behavior of the voltage near the KT phase transition is of the general form

$$\langle V\rangle = iA_1 \exp[A_2/(T-T_{\rm KT})^{1/2}] , \tag{13}$$

where A_1 and A_2 are parameters.[26] At the Kosterlitz-Thouless phase transition the voltage is produced by the appearance and dissociation of vortex-antivortex pairs which are seen in the numerical simulations discussed below.

Finally, in a disordered array with many defects and an applied bias current there are many vortices and antivortices pinned to the defects in a state of self-organized criticality[14,15] which are easily shaken loose by the thermal fluctuations or by an applied ac current and thus $T_{\rm KT}$ is greatly reduced and the photoresponse is enhanced.

In order to make the connection between the various below-gap experimental results and our numerical simulations we define the photoresponse as the voltage change across the sample

$$\Delta V_R(i_{\rm dc},i_{\rm ac},f,T) \equiv \langle V(i_{\rm dc},i_{\rm ac},f,T)\rangle - \langle V(i_{\rm dc},0,0,T)\rangle \tag{14}$$

produced by the applied ac current.

III. NUMERICAL SIMULATIONS

The photoresponse of thin-film superconductors is typified by the results of Strom *et al.*[10] from thin films of YBCO. As a function of temperature the photoresponse ΔV_R shows a nonbolometric peak (see, for example, Figs. 5 and 6, of Ref. 10) at low temperature which increases in magnitude with increased $i_{\rm dc}$, $i_{\rm ac}$ and which moves to lower temperature and increases in magnitude with decreasing frequency of the applied radiation. The peak is especially strong for granular and disordered samples.

In order to better understand our calculations we begin with the photoresponse of a single junction. First, we apply a white-noise current $\tilde{i}(t)$ according to the prescription in Eqs. (1) and (2) with a different random current distribution in each time step. Then we apply a bias current $i_{\rm dc}$ across the junction and integrate to solve the differential equation (5). The results of this numerical procedure are shown as the data points in Fig. 2 where the dotted line corresponds to Ambegaokar and Halperin's analytic solution[20] for a single junction as given by Eq. (10) for $i_{\rm dc}=0.1$, 0.2, and 0.4. Then we add an ac current of magnitude $i_{\rm ac}$ and frequency f as in Eq. (8) and repeat the process to solve Eq. (5) with the result shown in Fig. 3 for $f=0.1$ and 0.5 (in units of $\hbar/eJR$). There is clearly a peak in each of the photoresponse curves of Fig. 3 corresponding to the fact that as the ac current is applied the rise of the voltage to its limiting value ($i_{\rm dc}R$) is pushed to lower temperatures. There is a larger photoresponse at lower frequencies. Next, we con-

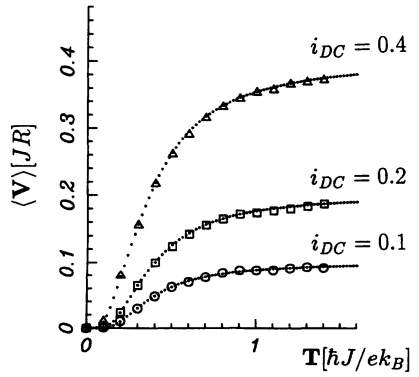

FIG. 2. Plots of $\langle V\rangle$ vs temperature T for a single Josephson junction for the bias current $i_{\rm dc}=0.1$, 0.2, and 0.4. The symbols represent the numerical solution of Eq. (5), the dotted curve represents the analytic solution in Eq. (10).

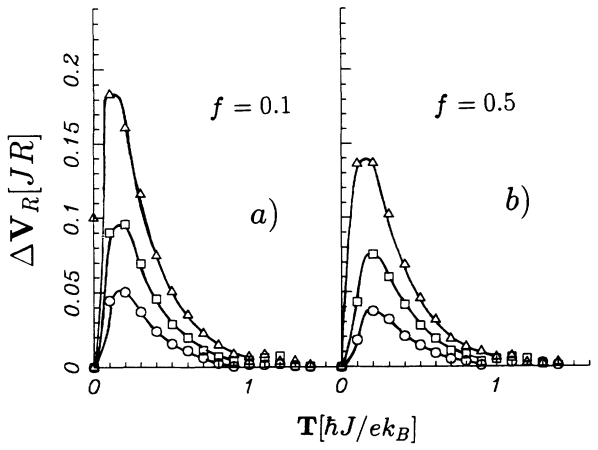

FIG. 3. Plots of photoresponse ΔV_R of a single Josephson junction vs temperature T for $i_{\rm dc}=0.1$, 0.2, and 0.4, and for (a) $f=0.1$, and (b) $f=0.5$. The applied ac current magnitude is $i_{\rm ac}=0.8$.

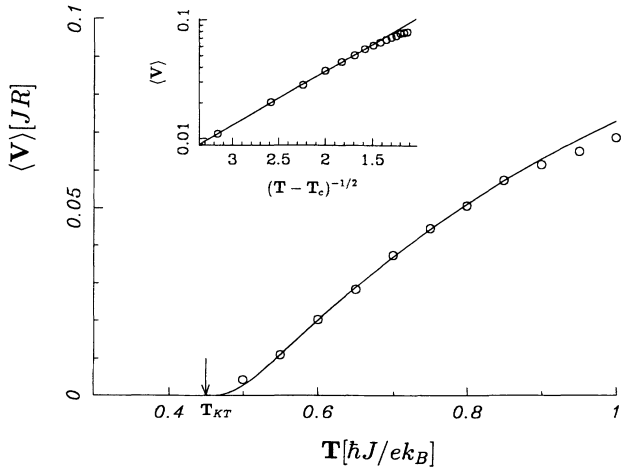

FIG. 4. A plot of $\langle V\rangle$ vs temperature T for a 16×16 perfect array of RSJ junctions. The circles are the numerical solution of Eqs. (11) or (12), while the solid line is a fit to (13) with $T_{\rm KT}=0.45$, $A_1=3.01$, and $A_2=1.05$. The bias current is $i_{\rm dc}=0.1$. Inset: A semilog plot of $\langle V\rangle$ vs $(T-T_{\rm KT})^{-1/2}$.

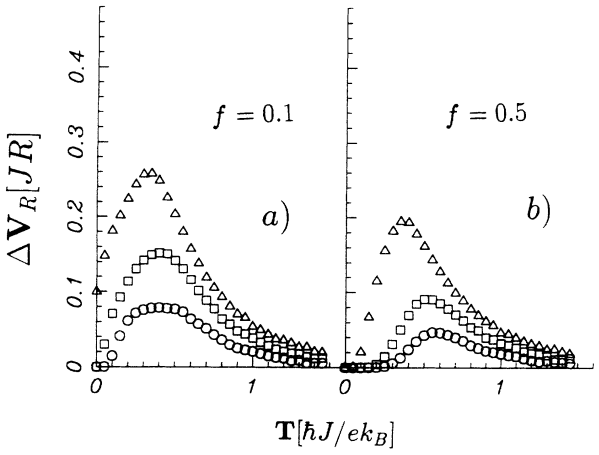

FIG. 5. Plots of the photoresponse ΔV_R vs T for a perfect 8×8 RSJ junction array for $i_{dc}=0.1$, 0.2, and 0.4, and (a) $f=0.1$, and (b) $f=0.5$. The value of $i_{ac}=0.8$.

sider a perfect $N\times N$ array of junctions, applying the external current to the bus bar sites on the top and bottom of the array, as shown in Fig. 1.

First, we confirm the earlier results of Mon and Teitel[17] and Chung, Lee, and Stroud,[18] which show the Kosterlitz-Thouless transitions for the perfect array. We solve the coupled set of nonlinear differential equations (11) or actually the matrix equation (12) by applying a bias current i_{dc} and a white-noise current $\tilde{i}(t)$ randomly to each site with the result shown in Fig. 4 where it is confirmed that our results agree with Eq. (13) (solid line) with $T_{KT}=0.45$. Then, the ac current is added to the external current as in Eq. (8) with the resulting photoresponse shown in Fig. 5. The peak in the photoresponse has been shifted to higher temperature relative to that for a single junction (Fig. 3) as the cooperative effects of the coupled junctions serve to suppress the fluctuation to higher temperatures. Actually the peak in the photoresponse versus temperature shifts to $T_{KT}=0.45$ in the limit as $i_{dc}\to0$. As the bias current is increased the peak shifts to lower temperature and indeed the curve remains finite at $T=0$ when the bias current exceeds the critical current for the first Shapiro step in the voltage. The magnitude of the photoresponse per junction in the array is greater than that for a single junction due to the creation of vortex-antivortex pairs in the array. In Fig. 6, we plot the photoresponse versus bias current i_{dc} for three different temperatures $T=0.25$, 0.45, and 0.85. For low temperatures the photoresponse is very small until the bias current nears the first Shapiro step. At $T>T_{KT}$ there is an initial linear region versus bias current followed by a saturation.

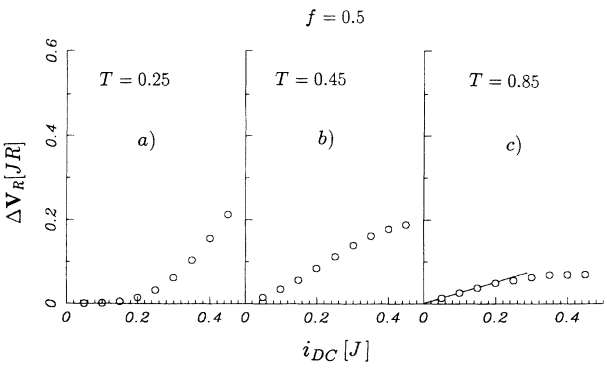

FIG. 6. The photoresponse ΔV_R vs i_{dc} for (a) $T=0.25$, (b) $T=0.45$, and (c) $T=0.85$ for a perfect 8×8 RSJ junction array. The value of $i_{ac}=0.8$.

A mechanism for the production of vortex-antivortex pairs by the applied external field has, for the above-gap case, been suggested by Kadin *et al.*,[4] but we have observed a very similar mechanism for the below-gap response. The mechanism we have seen in these simulations is illustrated in Fig. 7 and is as follows. First there is a large random temperature fluctuation. In our simulations this appears as a large current fluctuation which may be in the direction of the applied bias current. If this random current fluctuation makes the total current in the region to be near or above the critical current then the excess current caused by the ac current (or the dc current near T_{KT}) is shunted to each side of the fluctuation, as is illustrated in Fig. 7(a), just as if the fluctuation were a defect.[14,15] This sweeping of the current around the ends of the fluctuation creates a vortex and an antivortex on the opposite ends of the fluctuation, as it would about a defect.[14,15] The bias current then sweeps the vortex and antivortex across the sample in opposite directions creating the photoresponse voltage. An example of this process is shown in Fig. 8 for a 16×16 perfect array. In this example, the temperature fluctuation at Monte Carlo time step $t=28\,080$ creates a current enhancement on each end which evolves into a separate vortex and antivortex, and these vortices then move away from each other across the sample perpendicular to the external current annihilating each other when they meet, due to the periodic boundary conditions. This series of snapshots was taken at a low temperature $T=0.025$ in order to isolate a single vortex-antivortex pair; at higher temperatures the number of such pairs increases and

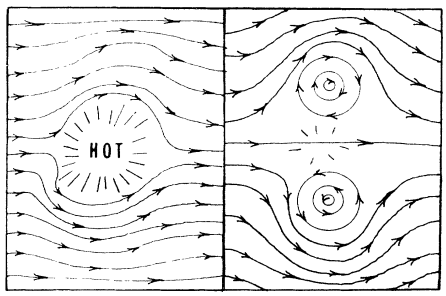

FIG. 7. A schematic picture of the creation of vortex-antivortex pairs by the temperature fluctuations, i_{dc}, and i_{ac}. The current flow produced by $i_{dc}+i_{ac}$ flowing past a high-temperature fluctuation is diverted around it, as if it were a defect, creating a vortex and an antivortex on the opposite ends of the fluctuation which can be depaired by the applied current to move across the sample producing a voltage.

often many are present at any one time.

Finally, to simulate the granular, thin-film superconductors we repeated these simulations on disordered arrays of Josephson junctions. The arrays are disordered by the random removal of junctions (or bonds) as is typified by the sample shown in Fig. 9. When a bias current is passed through such disordered samples there are emerging vortices and antivortices pinned to the ends of each random defect. As the bias current is increased, more and more of the sample is in a state of self-organized criticality,[14,15] just on the verge of releasing the local vortices from their pinning sites. So when the ac current is applied a much larger response is seen at low temperatures due to presence of disorder.

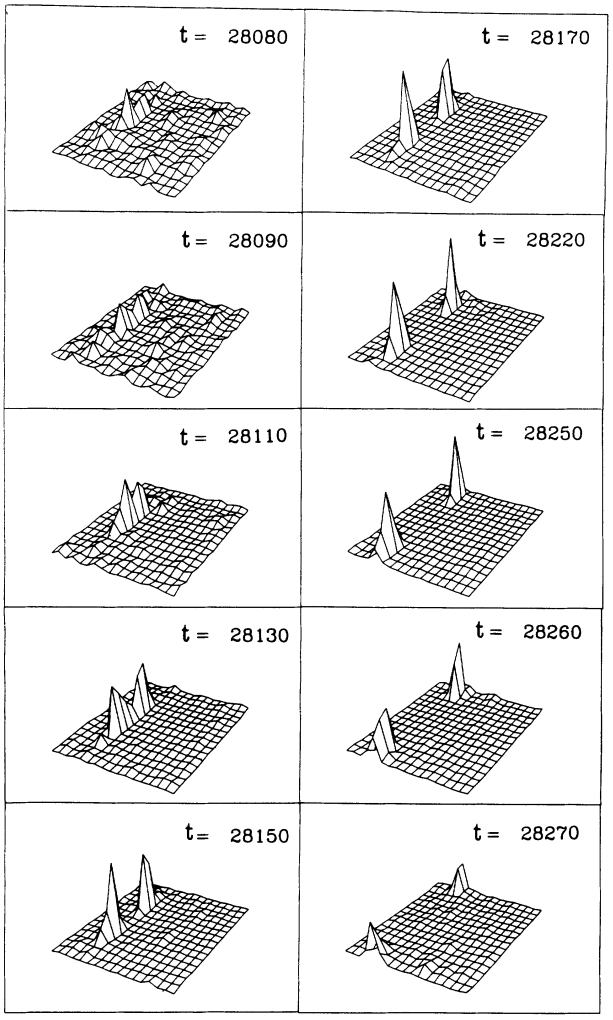

FIG. 8. Snapshots of the creation and annihilation of a vortex-antivortex pair in a perfect 16×16 array at $T=0.25$, $i_{dc}=0.7$, $i_{ac}=0.25$, and $f=0.2$. The Monte Carlo time steps are indicated on each picture as the temperature fluctuation produces a barrier to the super current flow which causes the vortex and antivortex to be produced on each end of the fluctuation to depin, and travel across the sample annihilating at the periodic boundary conditions. The actual plot is of the magnitude of the supercurrent flowing in the bonds perpendicular to the external current.

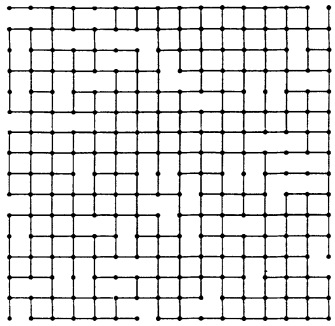

FIG. 9. A typical sample of RSJ junctions in a 25×25 array with $p=0.90$ so that 10% of the bonds are vacant.

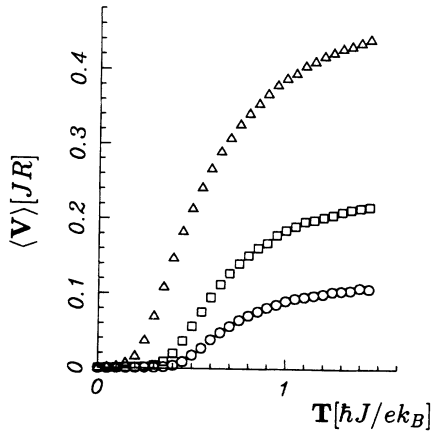

FIG. 10. The average voltage $\langle V\rangle$ vs T for an 8×8 disordered ($p=0.90$) RSJ junction array for $i_{dc}=0.1$, 0.2, and 0.4.

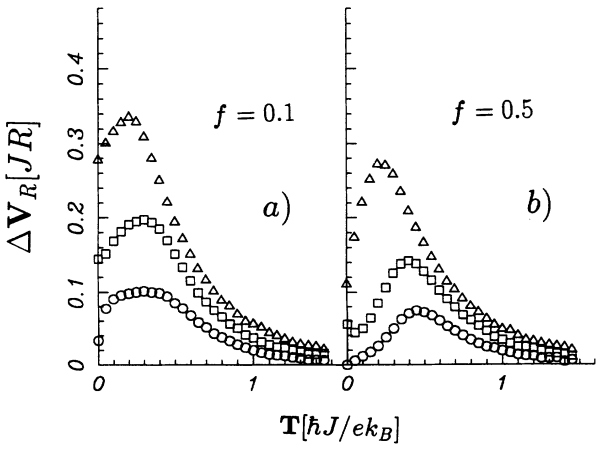

FIG. 11. The photoresponse ΔV_R vs T for an 8×8 disordered ($p=0.90$) array of RSJ junctions with $i_{dc}=0.1$, 0.2, and 0.4, and (a) $f=0.1$, and (b) $f=0.5$, with $i_{ac}=0.8$.

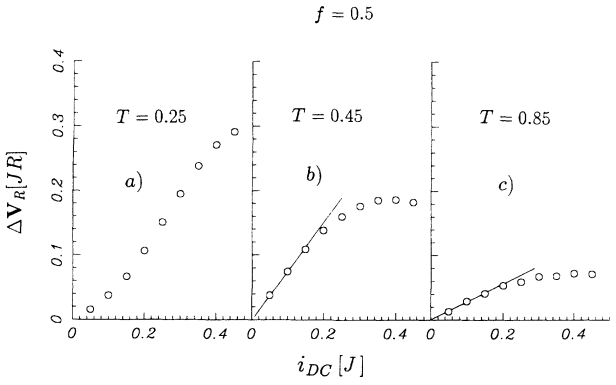

FIG. 12. The photoresponse ΔV_R vs i_{dc} for an 8×8 disordered ($p=0.90$) array for (a) $T=0.25$, (b) $T=0.45$, and (c) $T=0.85$, with $i_{ac}=0.8$ and $f=0.5$.

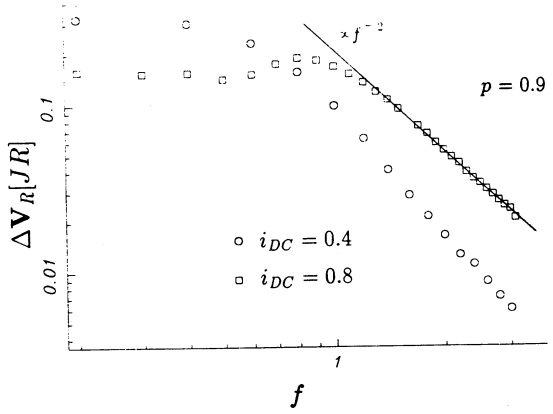

FIG. 14. The photoresponse ΔV_R vs f, for $i_{dc}=0.4$ and 0.8, with $i_{ac}=0.8$, and $T=0.2$ in 8×8 disordered arrays ($p=0.90$). For $i_{dc}=0.8$, ΔV_R goes to zero as f^{-2} at high frequency in this model.

The voltage vs temperature is shown in Fig. 10 for three values of the bias current $i_{dc}=0.1$, 0.2, and 0.4. When the ac current is added the photoresponse is as shown in Figs. 11(a) and 11(b). Here the photoresponse is considerably larger than that shown in Fig. 6 for the perfect array. The peak in the response is at lower temperatures in the disordered arrays due to the lowered Kosterlitz-Thouless transition temperature and moves to still lower temperatures as the bias current i_{dc} is increased. These peaks in Fig. 11 are qualitatively very like those seen in the experiments on thin-film superconductors (see, for example, Figs. 5 and 6 of Strom *et al.*[10]).

We have also calculated the behavior of the photoresponse vs bias current with the results shown in Fig. 12 for $T=0.25$, $T=0.45=T_{KT}$, and $T=0.85$ (for comparison with Fig. 7 of Strom *et al.*[10]). There is good qualitative agreement between these simulations and the experiments if one assumes that the bias current in the real experiments did not exceed about $i_{dc}=0.3$. At these lower values of i_{dc}, the photoresponse curves upward vs i_{dc} for $T=0.25$ corresponding to the remnant of the onset of the first Shapiro step, whereas for $T\gtrsim T_{KT}=0.45$ the photoresponse vs i_{dc} is linear for $I_{dc}\lesssim 0.3$. These re-

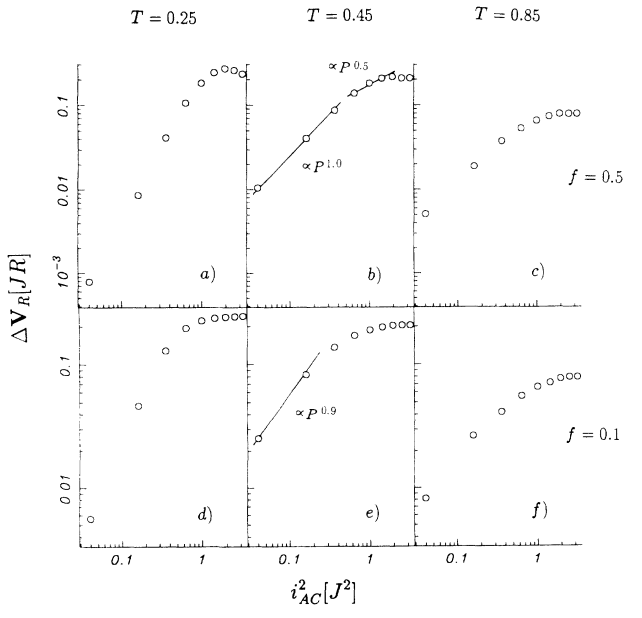

FIG. 13. The photoresponse ΔV_R vs i_{ac}^2 for an 8×8 disordered ($p=0.90$) array of RSJ junctions with $T=0.25$ in (a) and (d), $T=0.45$ in (b) and (e), and $T=0.85$ in (c) and (f), and where $f=0.5$ in (a), (b), and (c), and $f=0.1$ in (d), (e), and (f). The value of $i_{dc}=0.4$.

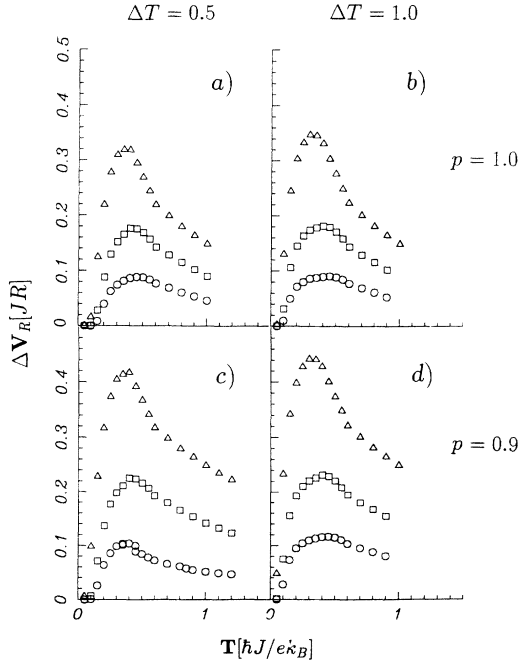

FIG. 15. A simulation of above-gap photoresponse ΔV_R vs T for an 8×8 RSJ junction array with 10% of the junctions heated by $\Delta T=0.5$ [in (a) and (c)] and $\Delta T=1.0$ [in (b) and (d)] randomly in each Monte Carlo time step. The curves are for $i_{dc}=0.1$, 0.2, and 0.4. (a) and (b) are for a perfect array ($p=1.0$), while (c) and (d) are for a disordered array ($p=0.9$).

sults are much more like the behavior seen experimentally (especially at $T=0.25$) than are the results for the perfect array (Fig. 6) which shows very little photoresponse at low values of i_{dc}.

Another comparison is with the photoresponse vs incident power (i_{ac}^2) for the disordered array. These numerical results are shown in Fig. 13 for $T=0.25$, 0.45, and $T=0.85$ and for $f=0.5$ and 0.1. Figures 13(b) and 13(e), where $T=T_{KT}$, are to be compared with Fig. 8 of Strom *et al.*[10] for $i_{ac}^2 \lesssim 1.0$. Strom *et al.* have fit these curves to straight line power laws and that can be done here with about the same degree of success as is seen by the straight lines in Figs. 13(b) and 13(e). But we do not really believe that these curves are simple power laws. For the record, we plot in Fig. 14, the photoresponse versus frequency f for the disordered samples at $i_{dc}=0.4$, and 0.8. These curves clearly drop off rapidly at high frequencies. The drop at high frequencies becomes less steep as the current i_{dc} is increased until the i/f^2 high-frequency behavior of single junctions [Eq. (9)] is seen at about $i_{dc}=0.8$. This is not what one would expect as the high-frequency limit in real experiments because this limit is above the superconducting energy gap and something more like the f^{-1} suggested by Kadin *et al.*[4] would seem more appropriate here as individual photons separate Cooper pairs.

Finally, we report a brief attempt to simulate the above-gap response by randomly heating isolated sites in the lattice in each time step to mimic the effect of pair breaking by the photons. The results for the photoresponse versus temperature are shown in Fig. 15 for both the perfect ($p=1.0$) and disordered ($p=0.9$) arrays where 10% of the sites are randomly raised upward in temperature by $\Delta T=0.5$, or 1.0 in each Monte Carlo time step. This procedure clearly creates extra vortex-antivortex pairs and hence a photoresponse. The results are qualitatively like those reported by Strom *et al.*[10] but we have not pursued this model further.

IV. CONCLUSION

The below-gap photoresponse seen experimentally in many granular and disordered thin-film superconductors can be simulated by applying an ac current at finite temperature to two-dimensional disordered arrays of resistively shunted Josephson junctions. Virtually all of the qualitative features seen experimentally are reproduced in this manner. This agreement makes it very clear that the photoresponse is generated by the depairing and depinning of vortex-antivortex pairs by the combination of the temperature, the bias current and the applied ac current. Explicit analytic calculations should now be done using the models identified here to understand quantitatively these photoresponse phenomena.

ACKNOWLEDGMENTS

We would especially like to thank Dr. Ulrich Strom for suggesting this calculation and for his very helpful discussions and suggestions. We also acknowledge useful conversations with Philip Duxbury and Chris Lobb on this calculation. We should like to thank the Department of Physics and Astronomy of Michigan State University, where much of this work was done. The authors also gratefully acknowledge the CAIP Center at Rutgers and the NCUBE Corporation for the access to their NCUBE systems. And finally we acknowledge a vital grant of computing time on the Cray-YMP at the NSF Pittsburgh Supercomputing Center without which this project could not have been done.

[1]C. L. Bertin and K. Rose, J. Appl. Phys. **42**, 631 (1971).
[2]N. Fujimaki, Y. Okabe, and S. Okamura, J. Appl. Phys. **52**, 912 (1981).
[3]G. L. Carr, D. R. Karecki, and S. Perkowitz, J. Appl. Phys. **55**, 3892 (1984).
[4]A. M. Kadin, M. Leung, A. D. Smith, and J. M. Murduck, Appl. Phys. Lett. **57**, 2847 (1990).
[5]M. Leung, U. Strom, J. C. Culbertson, J. H. Claassen, S. A. Wolf, and R. W. Simon, Appl. Phys. Lett. **50**, 1691 (1987); U. Strom, J. C. Culbertson, S. A. Wolf, S. Perkowitz, and G. L. Carr, Phys. Rev. B **42**, 4059 (1990).
[6]Y. Enomoto and T. Murakami, J. Appl. Phys. **59**, 3807 (1986); Y. Enomoto, Y. Murakami, and M. Suzuki, Physica C **153-155**, 1592 (1988).
[7]P. G. Huggard, Gi. Schneider, T. O'Brien, P. Lemoine, W. Blau, and W. Prettl, Appl. Phys. Lett. **58**, 2549 (1991).
[8]M. Leung, P. R. Broussard, J. H. Claussen, M. Osolsky, S. A. Wolf, and U. Strom, Appl. Phys. Lett. **51**, 2046 (1987); J. C. Culbertson, U. Strom, S. A. Wolf, P. Skeath, E. J. West, and W. Burns, Phys. Rev. B **39**, 12 359 (1989).
[9]J. C. Culbertson, U. Strom, S. A. Wolf, and W. W. Fuller, Phys. Rev. B **44**, 9609 (1991).
[10]U. Strom, J. C. Culbertson, S. A. Wolf, F. Gao, D. B. Tanner, and G. L. Carr, Phys. Rev. **46**, 8472 (1992).
[11]F. Guinea and G. Schön, Physica B **152**, 165 (1988).
[12]C. J. Lobb, D. W. Abraham, and M. Tinkham, Phys. Rev. B **27**, 150 (1983).
[13]K. A. Müller, M. Takashige, and J. G. Bednorz, Phys. Rev. Lett. **58**, 1143 (1987); M. Tinkham, *ibid.* **61**, 1658 (1988); Y. Yeshurun and A. P. Malozemoff, *ibid.* **60**, 2202 (1988).
[14]W. Xia and P. L. Leath, Phys. Rev. Lett. **63**, 1428 (1989).
[15]P. L. Leath and W. Xia, Phys. Rev. B **44**, 9619 (1991).
[16]S. R. Shenoy, J. Phys. C **18**, 5163 (1985).
[17]K. K. Mon and S. Teitel, Phys. Rev. Lett. **62**, 673 (1988).
[18]J. S. Chung, K. H. Lee, and D. Stroud, Phys. Rev. B **40**, 6570 (1989).
[19]Ch. Leemann, Ph. Lerch, B. A. Racine, and P. Martinoli, Phys. Rev. Lett. **56**, 1291 (1986); R. K. Brown and J. C. Garland, Phys. Rev. B **33**, 7827 (1986); B. J. van Wees, H. S. J. van der Zant, and J. E. Mooij, *ibid.* **35**, 7291 (1987); M. G. Forrester, H. J. Lee, M. Tinkham, and C. J. Lobb, *ibid.* **37**, 5966 (1988); also see the conference proceedings, edited by J. E. Mooij and G. B. J. Schön, Physica B **152**, 1–302 (1988); D. J. Resnick, J. C. Garland, J. T. Boyd, S. Shoemaker, and R. S. Newrock, Phys. Rev. Lett. **47**, 1542 (1981); M. Tinkham, D. W. Abraham, and C. J. Lobb, Phys. Rev. B **26**, 6578 (1983); R. A. Webb, R. F. Voss, G. Grinstein, and P. M. Hom, Phys. Rev. Lett. **51**, 690 (1983); D. Kimhi, F. Leyvrayz, and D. Ariosa, Phys. Rev. B **29**, 1487 (1984).
[20]V. Ambegaokar and B. I. Halperin, Phys. Rev. Lett. **22**, 1364

(1969).
[21]For a good discussion of the single junction solution, see A. Barone and G. Paterno, *Physics and Applications of the Josephson Effect* (Wiley, New York, 1982).
[22]L. G. Aslamazov and A. I. Larkin, Pis'ma Zh. Eksp. Teor. Fiz. **9**, 150 (1969) [JETP Lett. **9**, 87 (1969)].
[23]H. Kanter and F. L. Vernon, Jr., J. Appl. Phys. **43**, 3176 (1972).
[24]B. I. Halperin and David R. Nelson, J. Low Temp. Phys. **36**, 1165 (1979).
[25]S. Doniach and B. A. Huberman, Phys. Rev. Lett. **42**, 1169 (1979).
[26]C. J. Lobb, David W. Abraham, and M. Tinkham, Phys. Rev. B **27**, 150 (1983).